Supporting Information for

Flexible client-dependent cages in the assembly landscape of the periplasmic

protease-chaperone DegP

Robert W. Harkness, Zev A. Ripstein, Justin M. Di Trani, and Lewis E. Kay

This PDF file includes:

Supporting text
Figures S1 to S8
Tables S1 to S4
SI References

Supporting Information Text

Materials and methods

Plasmid constructs and cloning

      The genes for expression of mature DegP (residues 27-474 lacking the periplasmic signal sequence and renumbered here as 1-448) and the DNA binding domain of human TRF1 (residues 378-430, renumbered here as 1-54 including an additional N-terminal Gly residue; see Table S1 for the construct sequence) were obtained as described previously[1]. The gene sequences for the chimeric clients TrpCage-hTRF1, IL6-hTRF1, and MNeon-hTRF1 were obtained by attaching the nucleotide sequence for hTRF1 to the 3' ends of the TrpCage, IL6, and MNeon genes respectively (see Table S1 for the protein sequences derived from these genes). We note that the His-SUMO-hTRF1 gene was not prepared in this manner as it could be produced by subcloning the sequence for hTRF1 into a plasmid backbone containing an N-terminal His_6-SUMO tag, as outlined below. For TrpCage-hTRF1 and His-SUMO-hTRF1, a linker sequence corresponding to a single Gly residue was included between the N-terminal protein and the C-terminal hTRF1 tag to allow for conformational freedom between the two domains of these chimeric clients. The genes for the chimeric constructs were synthesized as codon-optimized gBlocks® (Integrated DNA Technologies) containing 5' and 3' overhangs for subcloning. All expression constructs were prepared by subcloning the genes of interest using the Gibson Assembly® procedure (New England BioLabs Inc.) into kanamycin resistance pET plasmids with N-terminal His_6 affinity tags for purification. For MNeon-hTRF1, a pET29 plasmid was used with the N-terminal His_6 tag containing a C-terminal ENLYFQG motif that enabled cleavage of the affinity tag by TEV protease. All other constructs were subcloned into a *Champion* pET SUMO plasmid (hTRF1, TrpCage-hTRF1, IL6-hTRF1) which contains a sequence corresponding to an N-terminal His_6-

SUMO tag. The expression constructs for IL6 and MNeon were generated by mutating the first hTRF1 residue in the IL6-hTRF1 and MNeon-hTRF1 plasmids to a stop codon using the QuikChange site-directed mutagenesis method. Isolated TrpCage was not produced in this way; instead, it was obtained from GenScript as a synthetic peptide. It was not necessary to introduce a stop codon into the His-SUMO-hTRF1 construct to obtain a plasmid for expression of His-SUMO alone as this protein could be obtained during the purification of His-SUMO-hTRF1 as described in the following section.

Protein expression and purification

All proteins were expressed by growing transformed cells to an OD_{600} of ~0.6-1.0 at 37 °C in LB media at which point IPTG was added to 0.2 mM. Protein expression proceeded for a further ~16-20 hours at 23 °C, except for protease active DegP which was expressed for only 12 hours at 16 °C to mitigate autocatalysis. Other than DegP and IL6, all proteins were expressed in *Codon+ E. coli BL21(DE3)* cells. As DegP and IL6 contain native disulfide bonds[1,2], these proteins were expressed in *SHuffle T7 Competent E. coli cells* which produce disulfide isomerases that promote disulfide bond formation during cytoplasmic expression.

Protein purification proceeded in general according to (1) cell lysis and centrifugation, (2) nickel affinity chromatography, (3) His_6-SUMO tag cleavage, (4) an intermediate column chromatography step, and (5) size exclusion chromatography. For protease active DegP, all steps post-refolding from denaturing conditions (see below) were performed on ice or at 4 °C to diminish autocleavage. Cells were lysed on ice in lysis buffer (for most proteins this consisted of 100 mM NaH_2PO_4, 500 mM NaCl, pH 8.0; see below for exceptions) and subjected to centrifugation at 9000 rpm for 15 minutes to clear the lysate. Filtered supernatant was loaded onto a nickel affinity

purification column equilibrated with lysis buffer. The column was washed with buffer containing 10-30 mM imidazole pH 8.0 (3 rounds of 50-100 mL) to remove contaminant proteins. His$_6$-SUMO-tagged proteins of interest were eluted with lysis buffer containing 500 mM imidazole. For DegP, hTRF1, and TrpCage-hTRF1, the cell lysis and nickel chromatography steps were performed under denaturing conditions where 6M Gdn-HCl was included in the lysis buffer. This was implemented to remove bound substrates from DegP[1] and to protect hTRF1 and TrpCage-hTRF1 from protease cleavage in the earlier stages of the purification. DegP was eluted under denaturing conditions, while hTRF1 and TrpCage-hTRF1 were refolded on-column using a single five column volume wash step to 0M Gdn-HCl prior to elution with imidazole. DegP was subsequently refolded according to our previously published protocol[1]. His$_6$-SUMO tags were cleaved by incubation of the (refolded) elution fractions with Ulp1 protease for ~1 hour, except for His-SUMO-hTRF1 where the tag was left attached. Hydrophobic interaction chromatography was used as an intermediate purification step for DegP, IL6, and MNeon using a 5 mL Butyl HiTrap column according to our published method[1]. Briefly, nickel eluates were loaded onto the column after addition of solid ammonium sulfate to 1M. A stepped gradient from 1M to 0M ammonium sulfate in a base buffer of 25 mM NaH$_2$PO$_4$, 1 mM EDTA, pH 7.0 was used to elute the proteins of interest. Cation exchange chromatography was performed as an intermediate purification step for hTRF1, TrpCage-hTRF1, His-SUMO-hTRF1, IL6-hTRF1, and MNeon-hTRF1 using a 5 mL SP Sepharose column. The nickel eluates containing these proteins were diluted with buffer (25 mM NaH$_2$PO$_4$, 1 mM EDTA, pH 7.0) until the total salt concentrations were estimated to be lower than ~50-100 mM to ensure binding to the column. A gradient from 0 to 1M NaCl over five column volumes in a background of 25 mM NaH$_2$PO$_4$, 1 mM EDTA, pH 7.0 led to the elution of the protein of interest. Notably, for the proteins whose His$_6$-SUMO tags

were cleaved in a prior step by Ulp1 protease, this intermediate chromatography step permitted collection of the freed His_6-SUMO tags in the flow-through fraction, which could be independently gel-filtrated for use in the DLS control experiments (Figure S3). Elution fractions from the intermediate chromatography step were concentrated and subjected to size-exclusion chromatography in 25 mM NaH_2PO_4, 200 mM NaCl, 1 mM EDTA, pH 7.0 for final purification (30 mL format Superdex 75 and 200 Increase columns were used for client proteins and DegP respectively). In all cases, the purified proteins were buffer exchanged into the experimental buffer consisting of 25 mM NaH_2PO_4, 200 mM NaCl, 1 mM EDTA, pH 7.0 via Amicon Ultra concentrators. The concentrations of purified samples were calculated from their absorbances measured using a NanoDrop spectrophotometer (ThermoFisher) and their extinction coefficients at 280 nm (24 980, 31 970, 26 470, 35 200, and 69 330 M^{-1} cm^{-1} for hTRF1, TrpCage-hTRF1, His-SUMO-hTRF1, IL6-hTRF1, and MNeon-hTRF1 respectively) obtained from the ExPASY protein parameters calculator (https://web.expasy.org/protparam/protparam-doc.html). In order to reduce autocatalysis prior to use in activity assays, protease active DegP was lightly concentrated to 50 μM, aliquoted, flash frozen, and stored at -80 °C.

DLS measurements and autocorrelation analysis

DLS autocorrelation functions were measured using a plate reader format Wyatt DynaPro DLS instrument and analyzed according to the cumulants method to extract z-average diffusion constants (D_z) and polydispersity values as previously described[1,3,4]. Briefly, samples were prepared by dilution of concentrated protein stocks in a buffer of 25 mM NaH_2PO_4, 200 mM NaCl, 1 mM EDTA, pH 7.0. To remove contaminating dust, the experimental buffer was filtered (0.2 μm) and the sample tubes and the DLS plate wells were evacuated with compressed air prior to

use. Prior to loading on the DLS plate, samples were centrifuged at 17500 rpm for 15 minutes to pellet any large aggregates or dust. Wells containing 20 μL of each sample were capped with 10 μL infrared spectroscopy-grade paraffin oil to inhibit sample evaporation during the temperature ramp experiments. Experiments utilized S210A DegP at a protomer concentration of 100 μM and client concentrations of 50, 100, and 200 μM. Autocorrelation functions (averaged from 25 individual transients) for each sample well were recorded from 5-50 °C in 2.5 °C increments. The average autocorrelation functions were numerically fitted using in-house Python scripts to extract D_z and polydispersity values[1].

Protease activity assays

Crude activity assays were performed in 25 mM NaH_2PO_4, 200 mM NaCl, 1 mM EDTA, pH 7.0 by incubating 100 μM of the client proteins at 25 °C overnight in the absence and presence of 10 μM DegP. The reaction products were resolved by SDS-PAGE and stained with Coomassie Brilliant Blue for visualization. The gel image in Figure S4 was taken with a Bio-Rad GelDoc EZ imager. The reaction products were also subjected to liquid chromatography-mass spectrometry (LC-MS) analysis at the University of Toronto Department of Chemistry AIMS laboratory in order to identify cleavage fragments of hTRF1 derived from proteolysis by active DegP. The resultant masses corresponding to representative hTRF1 tag digestion products are indicated in Table S2.

Protease activity assays were additionally performed using changes in the intrinsic fluorescence of the hTRF1 tags of the clients as a reporter for cleavage by DegP. A Synergy Neo II plate reader (BioTek) with an excitation wavelength of 295 nm (slit width of 5 nm) and an emission wavelength of 335 nm (slit width of 10 nm) was used to measure the cleavage of the client proteins at 23 °C. Reactions were performed with 2.5 μM DegP and 25 μM substrate protein

in 100 μL volumes. Data were recorded at 1 minute intervals for a total of 50 minutes. Initial reaction velocities were obtained as the fitted slopes of the linear portions of the data corresponding to the first ~10-20 minutes of the experiment, depending on the substrate, and were corrected for photobleaching of the hTRF1 tag using an independent measurement of hTRF1 alone. Velocities shown in Figure 2E were normalized to the rate of cleavage of hTRF1 by DegP.

Single particle electron cryo-microscopy

(i)   *Preparation of electron cryo-microscopy samples*

To prepare proteins for imaging using cryo-EM, nanofabricated holey gold grids were glow discharged in air for 15 seconds, the samples were applied to the grids, and then the grids were blotted for between 15-20 seconds in a modified mark III FEI Vitrobot at 4 °C and ~100% humidity before plunge freezing in a 60:40 propane:ethane mixture held at liquid nitrogen temperature. For each sample, 2.5uL of protein in DLS buffer was applied to holey gold grids with a hole size of ~2 um. For all samples the S210A DegP protomer concentration was 100 μM, and each client protein (hTRF1, TrpCage-hTRF1, His-SUMO-hTRF1, IL6-hTRF1, and MNeon-hTRF1) was added in excess at 200 μM concentration.

(ii)   *Electron microscopy*

Datasets for S210A DegP in the presence of TrpCage-hTRF1, His-SUMO-hTRF1, and IL6-hTRF1 were collected on a FEI Tecnai F20 electron Microscope operating at 200 kV and equipped with a Gatan K2 summit direct detector device used in electron counting mode at 400 frames/sec. Movies were recorded as 30 fractions over a 15 second exposure. Defocuses ranged from ~1 to 3 μm. Movies were recorded at a nominal magnification of 25,000× corresponding to

a calibrated pixel size of 1.45 Å and with an exposure rate of ~5 electrons/pixel/s, and a total exposure of ~35 electrons/Å^2. A total of 166 (TrpCage-hTRF1), 119 (His-SUMO-hTRF1), and 189 (IL6-hTRF1) movies were collected using the Digital Micrograph software package.

For S210A DegP in the presence of hTRF1 and hTRF1-MNeon, datasets were collected on a Titan Krios G3 electron microscope (Thermo Fisher Scientific) operated at 300 kV and equipped with a prototype Falcon 4 direct detector device camera. Movies were recorded at a nominal magnification of 75,000× corresponding to a calibrated pixel size of 1.06 Å and with an exposure rate of ~5.5 electrons/pixel/s, and a total exposure of ~45 electrons/Å^2. 4,383 (hTRF1) and 1,185 (MNeon-hTRF1) movies were collected using the automated EPU software package. Movies were recorded as 29 exposure fractions over an 8.7 second exposure.

(iii)   Image analysis

All image analysis was carried out in *cryoSPARC* v3[5]. For all datasets patch-based alignment and exposure weighting was carried out and the resulting averages of frames were used for patch-based contrast transfer function (CTF) determination and particle picking. Templates for automated particle selection were generated by 2D classification of manually selected particles. The particle images obtained for S210A DegP in complex with hTRF1, TrpCage-hTRF1, His-SUMO-hTRF1, IL6-hTRF1, and MNeon-hTRF1 were extracted in 256×256, 256×256, 256×256, 360×360, and 512×512-pixel box sizes, respectively. Particle images for the His-SUMO-hTRF1, IL6-hTRF1, and MNeon-hTRF1 samples were Fourier cropped to 160×160, 180×180 and 256×256-pixel box sizes, respectively, prior to the refinements. After particle extraction, a combination of 2D classification and multi-class *Ab-initio* reconstruction was used to remove

broken particles, incorrect particle selections, and to classify particle images according to oligomer size (Figure 3A, Figure S5, and Figure S6).

Tree diagrams detailing the processing that led to the maps presented herein are shown in Figure S6. Briefly, the particle images from the *Ab-initio* classification of the hTRF1 dataset (with C_1 symmetry applied, equivalent to no symmetry group enforced) corresponding to a tetrahedral 12mer (483,190 particle images) were ultimately used in a refinement with enforced tetrahedral symmetry leading to a global resolution of 3.1Å. Subsequently, we performed symmetry expansion followed by local refinement with a mask over a portion of the molecule corresponding to a trimer, increasing the resolution to 2.6Å (Figure 5, Figure S6A, Figure S7A). Since the TrpCage-hTRF1 sample consisted mainly of 12mer particles, and because we were able to obtain a high resolution 12mer structure from the hTRF1 sample, no further analysis beyond multi-class *Ab-initio* reconstruction was performed on the TrpCage-hTRF1 dataset (Figure S6B). To generate the highest resolution maps of DegP oligomers from the His-SUMO-hTRF1, IL6-hTRF1, and MNeon-hTRF1 samples shown in Figure 3C, Figure S6C-E, and Figure S7B-D, the appropriate symmetry groups were enforced in refinements after confirming the symmetry of these species from *Ab-initio* reconstructions (with C_1 symmetry) and initial refinements with C_1 or other symmetries. For the His-SUMO-hTRF1 dataset, *Ab-initio* classes corresponding to the 18mer and 24mer (4,136 and 1,775 particle images, respectively) were used in refinements with enforced D_3 and octahedral symmetry respectively to generate maps with ~12 and ~14Å resolution. For the IL6-hTRF1 and hTRF1-MNeon datasets, *Ab-initio* classes corresponding to the 30mer and 60mer (5,592 and 14,443 particle images) were used in refinements with enforced D_5 and icosahedral symmetry respectively, yielding maps with ~14 and ~10Å resolution.

(iv)   Model Building

An atomic model for the client-engaged asymmetric unit of DegP consisting of a protease[i] domain, the hTRF1-bound PDZ1[i] domain from the same protomer, and an associated PDZ2[j] domain (*i* and *j* refer to protomers from separate trimers) was first built in *Coot*[6] using the 2.6Å map of the locally-refined hTRF1-bound DegP trimer. The asymmetric unit obtained from the crystal structure of a peptide-bound DegP 12mer (PDB 6JJO)[7] was used as a starting point for the model. We note that in our case, the hTRF1 strand is anchored to the PDZ1[i] domain via its C-terminus and extends to the protease[i] domain of an adjacent protomer that is not included in the asymmetric unit. The optimal asymmetric unit from *Coot* was then applied in a *Rosetta*[8] refinement where C_3 symmetry was imposed to generate a structural model of the hTRF1-bound DegP trimer. Statistics from this refinement are reported in Table S4. The 12mer, 18mer, 24mer, 30mer, and 60mer cage models were generated by propagating the refined hTRF1-bound trimer using the appropriate symmetry operations in *UCSF Chimera*[9]. Figures of maps and models were generated in *UCSF ChimeraX*[10].

Supporting Figures

A hTRF1 — $D_z = 2.24 \times 10^{-6}$ cm^2 s^{-1}, PD = 9%; hTRF1+DegP — $D_z = 4.32 \times 10^{-7}$ cm^2 s^{-1}, PD = 5%

B TrpCage-hTRF1 — $D_z = 5.13 \times 10^{-8}$ cm^2 s^{-1}; TrpCage-hTRF1+DegP — $D_z = 4.23 \times 10^{-7}$ cm^2 s^{-1}, PD = 4%

C His-SUMO-hTRF1 — $D_z = 1.15 \times 10^{-6}$ cm^2 s^{-1}, PD = 8%; His-SUMO-hTRF1+DegP — $D_z = 3.34 \times 10^{-7}$ cm^2 s^{-1}, PD = 6%

D IL6-hTRF1 — $D_z = 5.08 \times 10^{-9}$ cm^2 s^{-1}; IL6-hTRF1+DegP — $D_z = 2.42 \times 10^{-7}$ cm^2 s^{-1}, PD = 3%

E MNeon-hTRF1 — $D_z = 1.63 \times 10^{-8}$ cm^2 s^{-1}; MNeon-hTRF1+DegP — $D_z = 2.30 \times 10^{-7}$ cm^2 s^{-1}, PD = 15%
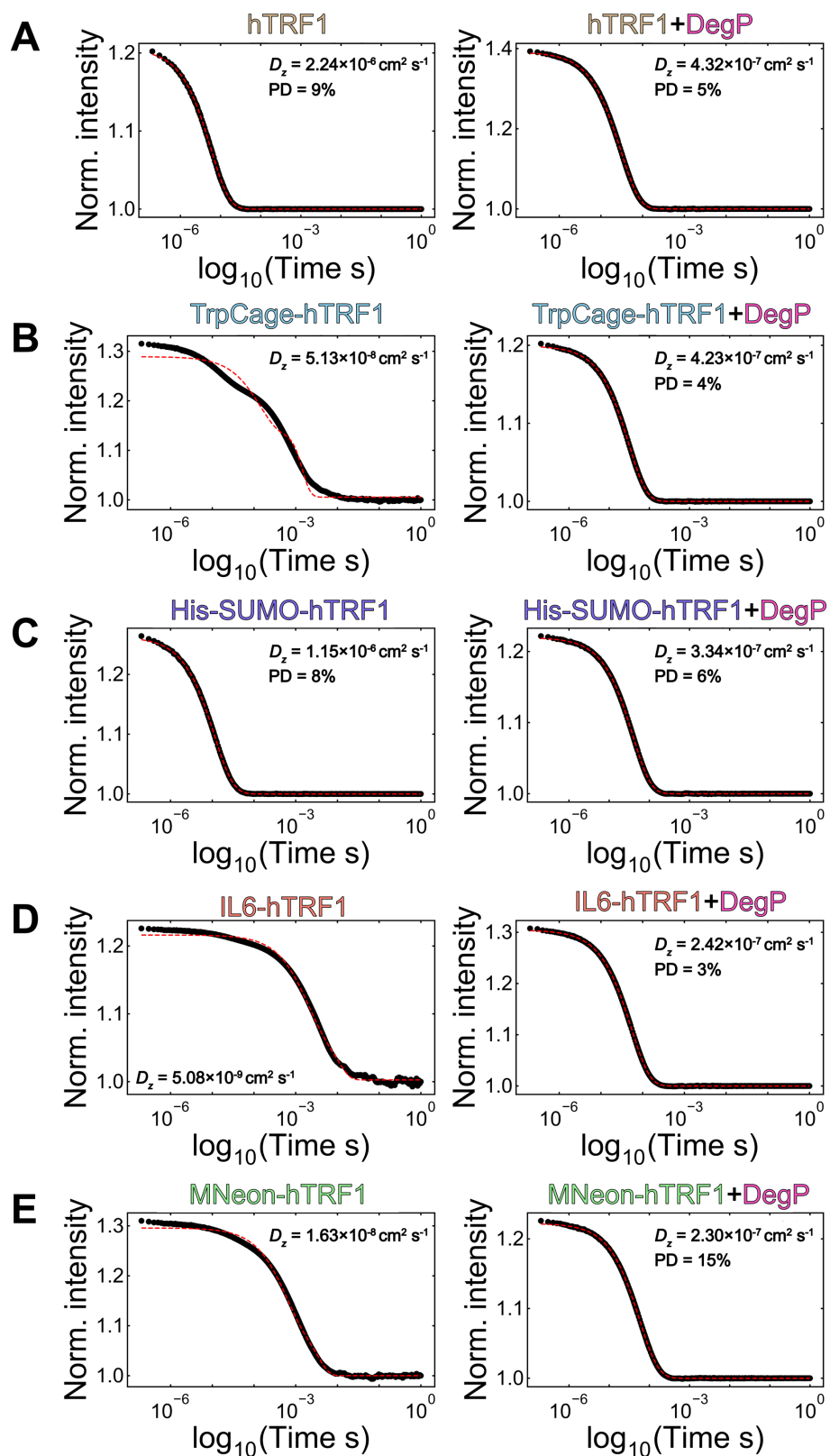
Figure S1. DLS autocorrelation data (black) for chimeric clients in the absence and presence of S210A DegP at 40 °C. (A-E, left) Autocorrelation data for apo hTRF1 (1200 μM), TrpCage-hTRF1 (1300 μM), His-SUMO-hTRF1 (250 μM), IL6-hTRF1 (300 μM), and MNeon-hTRF1 (400 μM) respectively. (A-E, right) Autocorrelation data for the substrates in (A-E, left) at 200 μM concentration bound to S210A DegP (100 μM). Higher protein concentrations were employed for the free clients in (A-E, left) in order to obtain accurate D_z values from their autocorrelation functions. Data were numerically fitted (red) using in-house Python scripts to extract D_z and polydispersity (PD) values[1]. The melting temperatures of hTRF1 and His-SUMO-hTRF1 (A, C, left) are within ~5 °C of the temperature used (40 °C), leading to a small fraction of the sample becoming denatured and somewhat elevated PD values. The poor fits for the TrpCage-hTRF1, IL6-hTRF1, and MNeon-hTRF1 datasets (B, D, E, left) are the result of sample aggregation that occurs at elevated temperatures, as discussed in the main text. PD values are not displayed for these samples as their particle distributions are inadequately described by this type of analysis at this temperature.
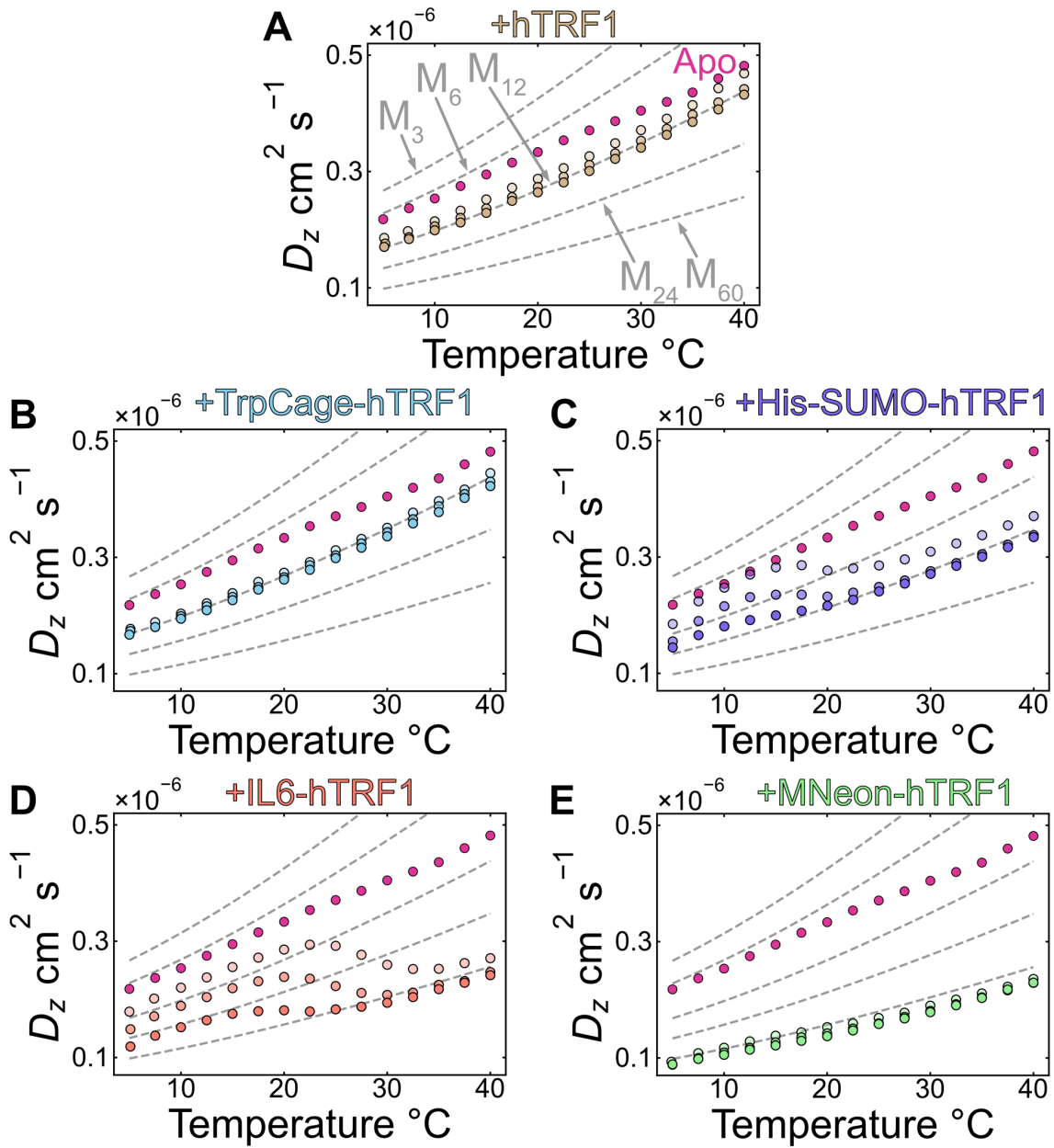
Figure S2. Characterizing DegP cages formed in the presence of the chimeric clients by DLS. (A-E) D_z values for 100 μM S210A DegP (monomer concentration) measured in the presence of 50, 100, and 200 μM client proteins (light to dark colored circles respectively). The client protein investigated in each experiment is indicated above the plots. D_z values for apo S210A DegP (red circles) are shown as a reference. D_0 values (grey dashed lines) calculated for 3mer, 6mer, 12mer,

24mer, and 60mer DegP particles are indicated. In the case of the 3mer, 6mer, and 12mer, r_hs of 4.9, 5.7, and 7.8 nm, respectively, were obtained from D_z values measured at low temperature[1], and then used to generate the D_0(T) profiles shown via the Stokes-Einstein equation. The profiles for the 24mer and 60mer oligomers were calculated from a scaling law for spherical particles that relates D_0(T) values to the number of DegP 3mers according to $D_{3N,0}$(T) = $D_{3,0}$(T)$\times N^{-1/3}$, where $D_{3,0}$(T) is the 3mer diffusion constant, N is the number of 3mers (=8 for the 24mer and 20 for the 60mer), and the -1/3 exponent accounts for the particle shape[1,11].
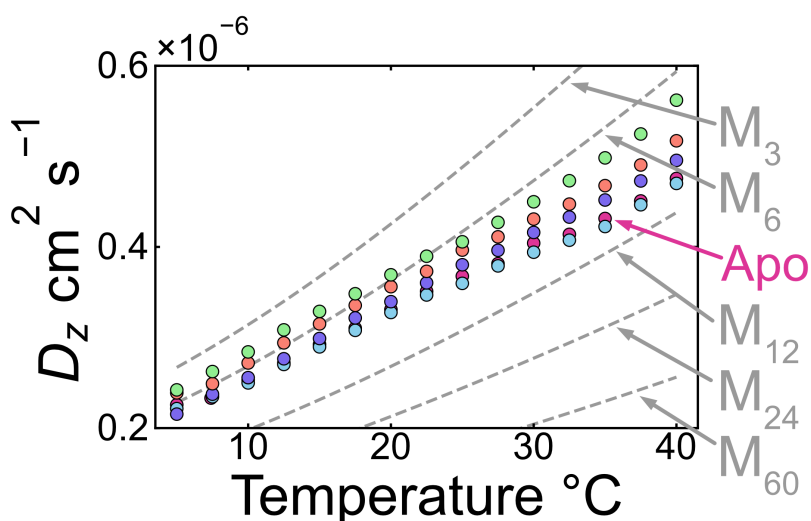

Figure S3. DLS analysis of DegP in the presence of the N-terminal portions of the chimeric clients. D_z values for apo S210A DegP, S210A DegP + TrpCage, S210A DegP + His-SUMO, S210A DegP + IL6, and S210A DegP + MNeon are shown as red, blue, purple, orange, and green circles respectively. Grey dashed lines corresponding to the diffusion constants for 3mer, 6mer, 12mer, 24mer, and 60mer particles have been simulated according to Figure 2 and Figure S2. These data were recorded with a 100 µM S210A DegP protomer concentration and 200 µM of each N-terminal fragment of the chimeric clients. Since D_z values are intensity-weighted averages over each

scatterer in solution (weighted by the molecular weight squared of each particle), in the absence of large cage formation, the smaller, unbound proteins in each well with DegP are expected to induce an upward shift in the D_z values. The D_z values recorded in the presence of these proteins reproduce the shape of the apo DegP profile (red circles) and are vertically shifted upward, indicating that no S210A DegP cages are formed. Note that the extent of the upward shifts increase as the size of the unbound clients grow, reflecting the molecular weight squared averaging of D_z.

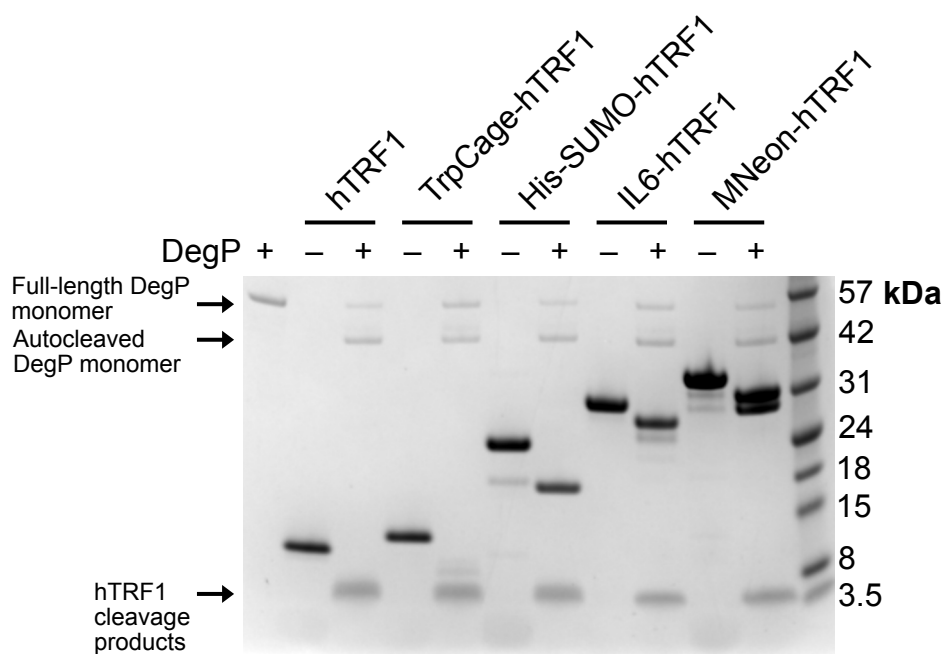**Figure S4.** Cleavage of hTRF1 and chimeric clients by DegP assayed by SDS-PAGE. DegP undergoes a slow autocleavage reaction in the presence of substrates, where its protease domain LA loop is partially digested[12], as evidenced by the band at ~42 kDa in the substrate lanes +DegP. Client cleavage products from the reactions in the presence of DegP are indicated by the arrow next to the molecular weight marker at ~3.5 kDa.
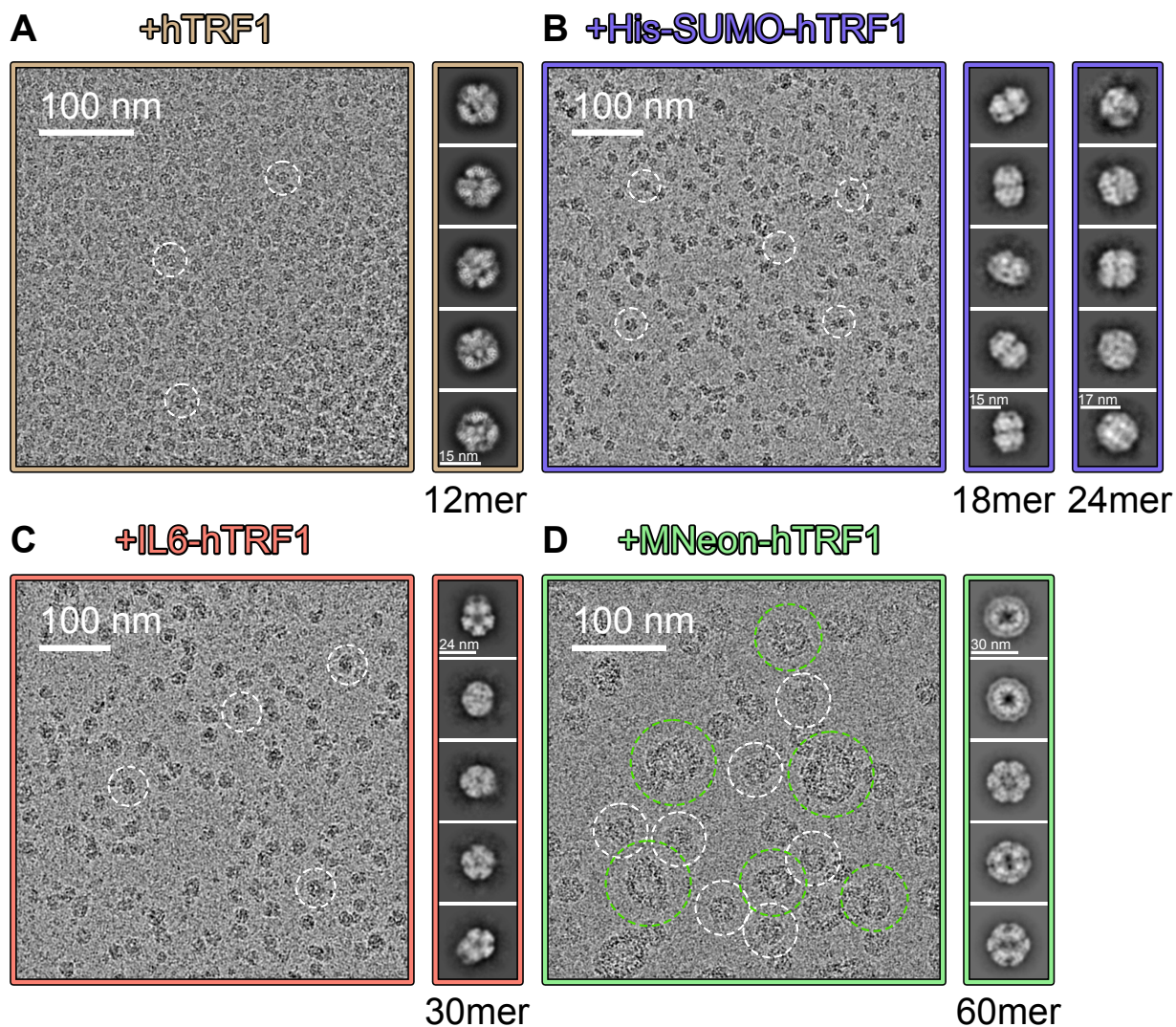
Figure S5. Micrographs and 2D class averages of DegP complexes that form in response to the engagement of the client proteins. Representative micrographs are shown for DegP cages that form in the presence of hTRF1 (A), His-SUMO-hTRF1 (B), IL6-hTRF1 (C), and MNeon-hTRF1 (D). 2D class averages for the DegP cage models that were constructed herein are shown to the right of the representative micrograph of the sample from which they were derived. Select particles within the micrographs are enclosed in white dashed circles. In (D), some of the extremely large DegP cages that form in the presence of MNeon-hTRF1 are encircled in green. A micrograph for DegP cages adopted in the presence of the TrpCage-hTRF1 client is not shown as these were found to

be nearly identical to those for the hTRF1 client in (A), except with a small fraction of 18mer particles (see main text). In order to better visualize the particles within the images, a bandpass filter and denoising and smoothing routines have been applied.

A +hTRF1

4,383 micrographs   **Titan Krios G3 electron microscope**

I. template picking based on manual selections, skip 2D classification

844,585 particles

Ab-initio reconstruction (C₁ symmetry), 3 classes

II.

15 nm

class 1, discarded, 307,926 particles

class 2, 12mer, (Figure 3B) 483,190 particles

class 3, discarded 53,469 particles

III. refine, C₁ symmetry   refine, T symmetry

15 nm

3.5Å resolution

3.1Å resolution (Figure 3C, Figure S7A)

IV. symmetry expansion   trimer local refinement
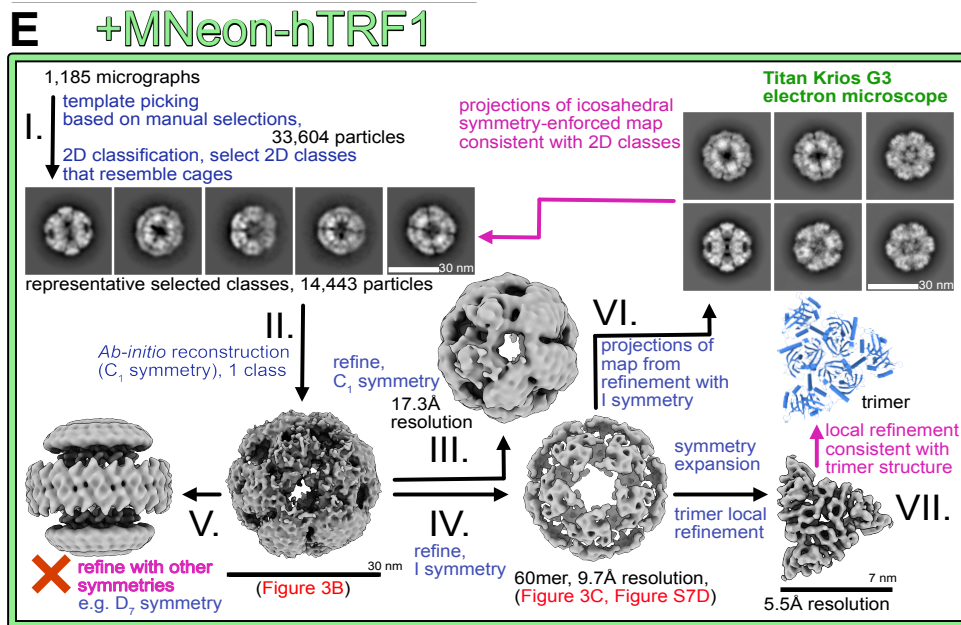

7 nm

2.6Å resolution (Figure 5, Figure S7A)

D +IL6-hTRF1

189 micrographs   **FEI Tecnai F20 electron microscope**

I. template picking based on manual selections,

13,646 particles

2D classification, select 2D classes that resemble cages

17 nm

representative selected classes, 7,852 particles

II. *Ab-initio* reconstruction (C₁ symmetry), 3 classes

17 nm   24 nm

III. refine, C₁ symmetry

class 1 & 2, 2,809 &1,947 particles, discarded

class 3, 30mer 3,096 particles (Figure 3B)

20.5Å resolution

IV. refine, D₅ symmetry

14.1Å resolution, (Figure 3C, Figure S7C)

B +TrpCage-hTRF1

166 micrographs   **FEI Tecnai F20 electron microscope**

I. template picking based on manual selections,

70,281 particles

2D classification, select 2D classes that resemble cages

15 nm

representative selected classes, 40,413 particles

II. *Ab-initio* reconstruction (C₁ symmetry), 3 classes

15 nm

class 1, 12mer 27,020 particles

class 2, discarded, 6,449 particles

class 3, discarded, 6,944 particles

C +His-SUMO-hTRF1

119 micrographs   **FEI Tecnai F20 electron microscope**

template picking based on manual selections

I. 35,366 particles   2D classification, make 3 classes based on 2D averages

15 nm

1,775 particles

4,136 particles   7,884 particles

Ab-initio reconstruction (C₁ symmetry)

II.

20 nm

15 nm   15 nm   17 nm

18mer (Figure 3B)   12mer   24mer (Figure 3B)

refine, C₁ symmetry   refine, D₃ symmetry   refine, O symmetry   refine, C₁ symmetry

III.

18.1Å resolution

20.1Å resolution

IV.

12.1Å resolution, (Figure 3C, Figure S7B)

13.8Å resolution, (Figure 3C, Figure S7B)

Figure S6. Cryo-EM image processing tree diagrams for the DegP:client complexes. The client added to DegP in each case is indicated above each panel. Note that for the DegP:hTRF1 dataset, it was possible to select for particle images corresponding to DegP oligomers and generate maps using *Ab-initio* reconstruction directly, alleviating the need for preliminary sorting of the particle images via 2D classification (note that representative 2D class averages are shown in Figure 3A and Figure S5A for comparison with the other complexes).
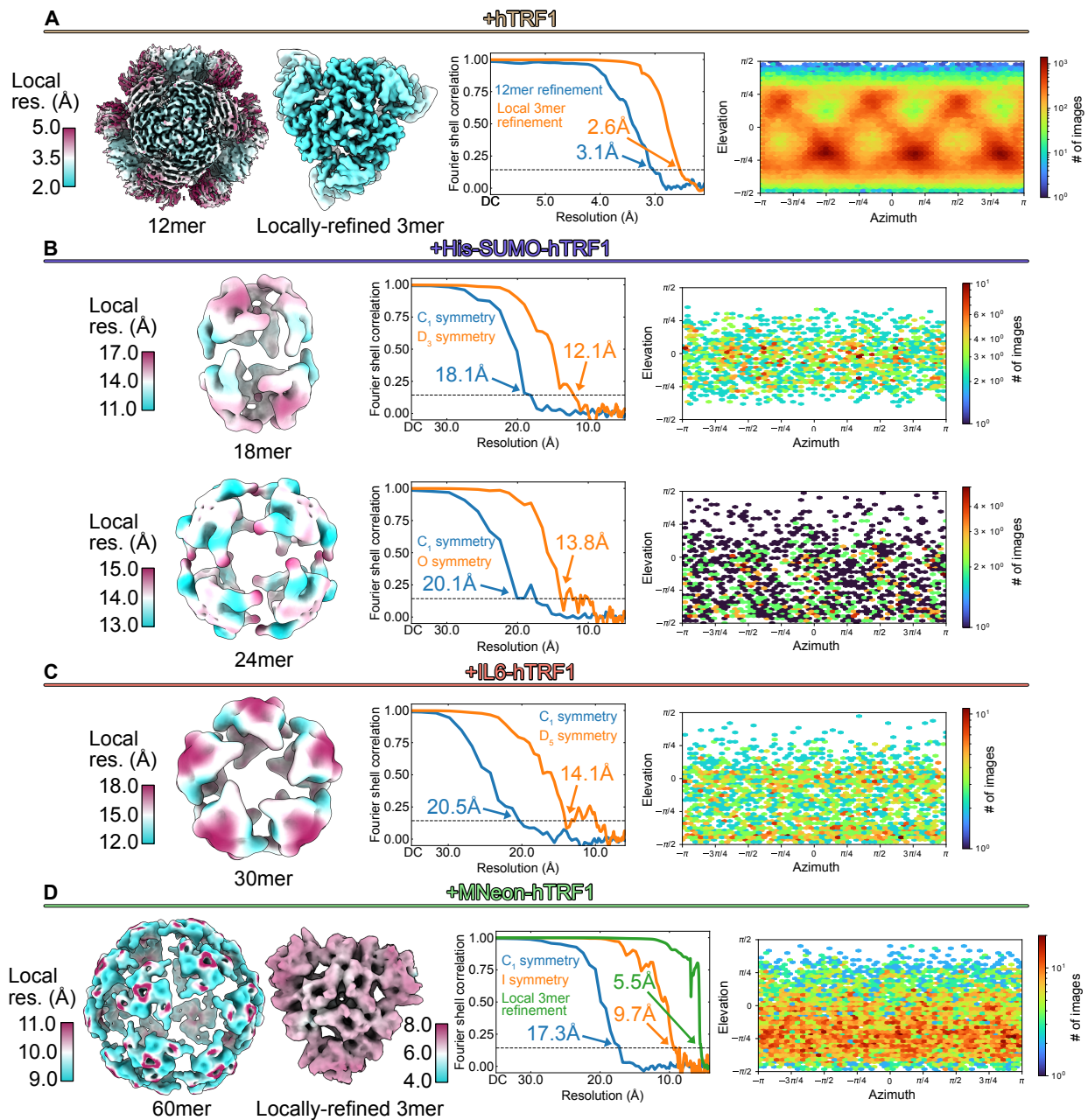
Figure S7. Cryo-EM maps of DegP cages adopted in the presence of clients. (A-D, left) Maps colored according to the local resolution for the 12mer and locally-refined trimer (hTRF1), 18mer and 24mer (His-SUMO-hTRF1), 30mer (IL6-hTRF1), and 60mer and locally-refined trimer (MNeon-hTRF1). (A-D, middle) Fourier shell correlation plots with global map resolution values. (A-D, right) Viewing direction distribution plots from the respective refinements in (A-D, left).
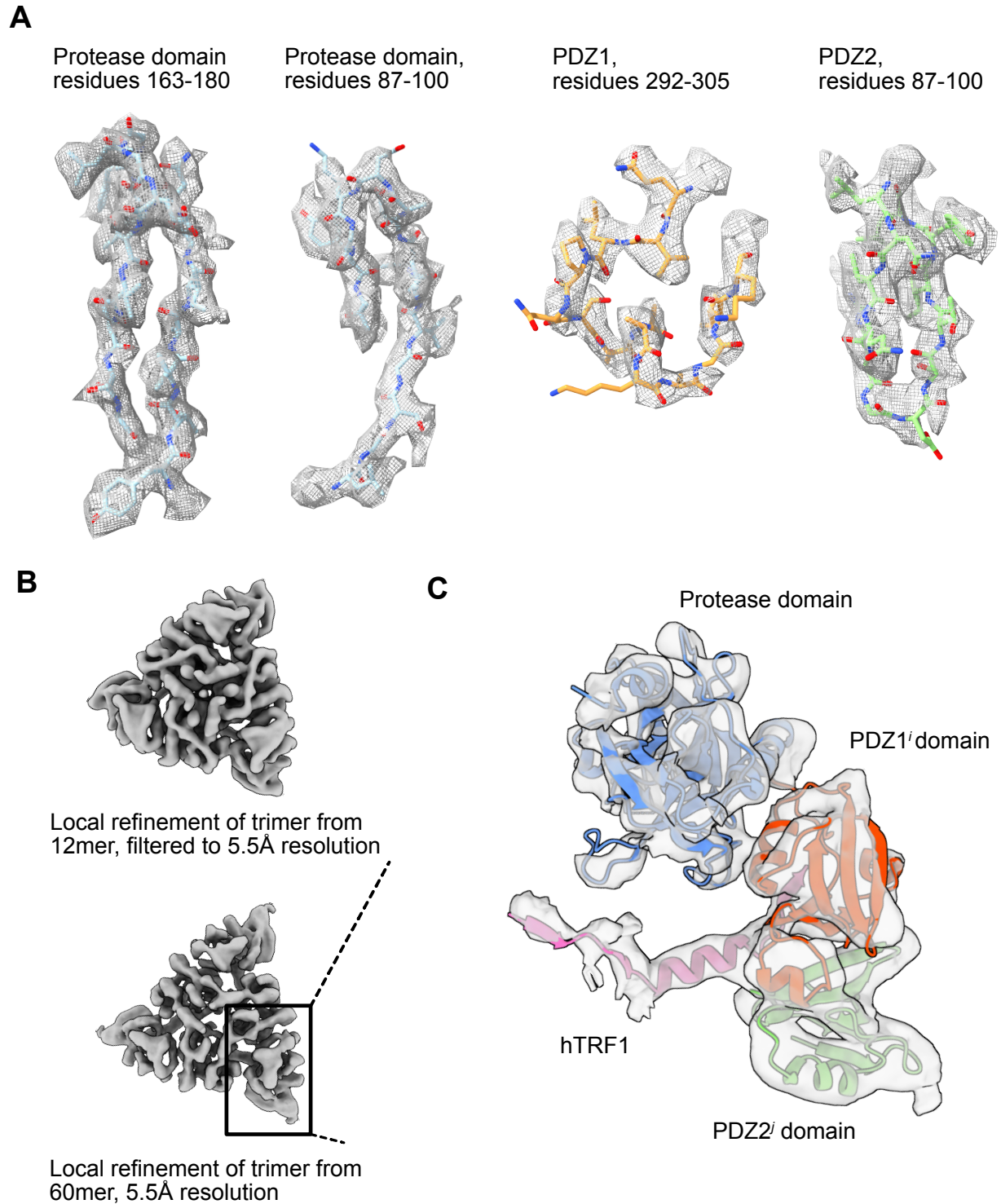
Figure S8. Model-in-map fits of the client-bound DegP trimer structure. (A) Representative model-in-map fits for the 2.6Å trimer local refinement map from the DegP:hTRF1 dataset. (B) Comparison of the trimer maps obtained from local refinements of the 12mer (hTRF1) and

approximately 60mer (MNeon-hTRF1) maps. Note that the trimer map obtained from local refinement of the 12mer map has been filtered to 5.5Å for direct comparison with that of the approximately 60mer map. (C) Atomic model of the trimer asymmetric unit, regions of which are shown in (A), rigid body fit into the corresponding portion of the MNeon-hTRF1 trimer local refinement map from (B). Density for the C-terminal half of the hTRF1 chain bridging the PDZ1 and protease domain binding sites is visible.

Supporting Tables

Table S1. Client protein amino acid sequences. The N-terminal domains of the chimeric clients are shown in black and their C-terminal hTRF1 tags are indicated in red.

Construct	Amino acid sequence
hTRF1	GRKRQAWLWEEDKNLRSGVRKYGEGNWSKILLHYKFNNRT SVMLKDRWRTMKKL
TrpCage-hTRF1	GNLYIQWLKDGGPSSGRPPPSGRKRQAWLWEEDKNLRSGVRKYGEGNWSK ILLHYKFNNRTSVMLKDRWRTMKKL
His-SUMO-hTRF1	MGSSHHHHHHSSGSDSEVNQEAKPEVKPEVKPETHINLKVSDGSSEIFFK IKKTTPLRRLMEAFAKRQGKEMDSLRFLYDGIRIQADQTPEDLDMEDNDI IEAHREQIGGGRKRQAWLWEEDKNLRSGVRKYGEGNWSKILLHYKFNNRT SVMLKDRWRTMKKL
IL6-hTRF1	GAPVPPGEDSKDVAAPHRQPLTSSERIDKQIRYILDGISALRKETCNKSN MCESSKEALAENNLNLPKMAEKDGCFQSGFNEETCLVKIITGLLEFEVYL EYLQNRFESSEEQARAVQMSTKVLIQFLQKKAKNLDAITTPDPTTNASLL TKLQAQNQWLQDMTTHLILRSFKEFLQSSLRALRQMRKRQAWLWEEDKNL RSGVRKYGEGNWSKILLHYKFNNRTSVMLKDRWRTMKKL
MNeon-hTRF1	GVSKGEEDNMASLPATHELHIFGSINGVDFDMVGQGTGNPNDGYEELNLK STKGDLQFSPWILVPHIGYGFHQYLPYPDGMSPFQAAMVDGSGYQVHRTM QFEDGASLTVNYRYTYEGSHIKGEAQVKGTGFPADGPVMTNSLTAADWCR SKKTYPNDKTIISTFKWSYTTGNGKRYRSTARTTYTFAKPMAANYLKNQP MYVFRKTELKHSKTELNFKEWQKAFTDVMGMDELYKRKRQAWLWEEDKNL RSGVRKYGEGNWSKILLHYKFNNRTSVMLKDRWRTMKKL

Table S2. Peptide masses and their corresponding sequences obtained from LC-MS analyses of cleavage products of hTRF1 and chimeric clients after proteolysis by active DegP. Masses were identified using the FindPept tool (https://web.expasy.org/findpept/) assuming a mass tolerance of 1.5 Da. The intact mass of hTRF1 and its corresponding sequence are shown in the top row of the table as a reference. Cleaved products are shown with their flanking residues in the intact hTRF1 chain in brackets. Note that for certain products, more than one fragment of hTRF1 can give rise to the observed mass at this level of detail (MS-MS is required for unambiguous sequence assignment) and thus multiple possible fragments are indicated in these cases. Since DegP processively digests the hTRF1 tag into many small fragments, as observed for other clients[13], only eight representative cleavage products are shown.

Mass (Dalton)	hTRF1 sequence(s)
6708.6	GRKRQAWLWEEDKNLRSGVRKYGEGNWSKILLHYKFNNRT SVMLKDRWRTMKKL
1078.5	(L)HYKFNNRT(S)
1264.6	(L)HYKFNNRTSV(M)
1304.7	(I)LLHYKFNNRT(S)
1490.8	(I)LLHYKFNNRTSV(M)
1492.8	(V)MLKDRWRTMKK(L) (S)GVRKYGEGNWSKI(L)
1604.9	(V)MLKDRWRTMKKL (S)GVRKYGEGNWSKIL(L)
1791.0	(T)SVMLKDRWRTMKKL
2949.5	(G)EGNWSKILLHYKFNNRTSVMLKDR(W) (G)NWSKILLHYKFNNRTSVMLKDRW(R) (A)WLWEEDKNLRSGVRKYGEGNWSKI(L) (S)KILLHYKFNNRTSVMLKDRWRTM(K) (K)ILLHYKFNNRTSVMLKDRWRTMK(K)

Table S3. Cryo-EM data acquisition and image processing.

TrpCage-hTRF1, His-SUMO-hTRF1 and IL6-hTRF1 Datasets			
Data Collection			
Electron Microscope	Tecnai F20		
Camera	Gatan K2 summit direct detector		
Voltage (kV)	200		
Nominal Magnification	25,000		
Calibrated physical pixel size (Å)	1.45		
Total exposure (e$^-$/Å^2)	~35		
Exposure rate (e$^-$/pixel/s)	~5		
Number of frames	30		
Defocus range (μm)	1 to 3		
Image Processing			
Motion correction software	*MotionCor2*		
CTF estimation software	*cryoSPARC v3*		
Particle selection software			
3D map classification and refinement software			
Sample	**TrpCage-hTRF1**	**His-SUMO-hTRF1**	**IL6-hTRF1**
Micrographs used	166*	119	189
Particle images selected	41,132*	35,366	7,417
hTRF1 and hTRF1-MNeon Datasets			
Data Collection			
Electron Microscope	Titan Krios		
Camera	Falcon 4		
Voltage (kV)	300		
Nominal Magnification	75,000		
Calibrated physical pixel size (Å)	1.06		
Total exposure (e$^-$/Å^2)	~45		
Exposure rate (e$^-$/pixel/s)	~5.5		
Number of frames	29		
Defocus range (μm)	0.9 to 2		
Image Processing			
Motion correction software	*MotionCor2*		
CTF estimation software	*cryoSPARC v3*		
Particle selection software			
3D map classification and refinement software			
Sample	**hTRF1**	**MNeon-hTRF1**	
Micrographs used	4,383	1,185	
Particle images selected	844,585	14,443	

*For the DegP:TrpCage-hTRF1 sample, the motion corrected micrographs were not subjected to further analysis beyond particle population estimates as they were determined to be mainly 12mer.

Table S4. Cryo-EM map and atomic model statistics.

Dataset	DegP:hTRF1 3mer local refinement
Modelling and refinement software	*Coot, Rosetta*
Protein residues	1212
Ligand	--
RMSD bond length (Å)	0.031
RMSD bond angle (°)	1.738
Ramachandran outliers (%)	0
Ramachandran favoured (%)	99.24
Rotamer outliers (%)	0
Clash score	0.44
MolProbability score	0.66
EMringer score	4.6

Supporting References

(1) Harkness, R. W.; Toyama, Y.; Ripstein, Z. A.; Zhao, H.; Sever, A. I. M.; Luan, Q.; Brady, J. P.; Clark, P. L.; Schuck, P.; Kay, L. E. Competing Stress-Dependent Oligomerization Pathways Regulate Self-Assembly of the Periplasmic Protease-Chaperone DegP. *Proceedings of the National Academy of Sciences of the United States of America* **2021**, *118* (32), 1–11. https://doi.org/10.1073/pnas.2109732118.

(2) Rock, F. L.; Klein, M.; Li, X.; Chong, P.; Ida, N. Roles of Disulfide Bonds in Recombinant Human Interleukin 6 Conformation. *Biochemistry* **1994**, *33* (17), 5146–5154. https://doi.org/10.1021/bi00183a018.

(3) Koppel, D. E. Analysis of Macromolecular Polydispersity in Intensity Correlation Spectroscopy: The Method of Cumulants. *The Journal of Chemical Physics* **1972**, *57* (11), 4814–4820. https://doi.org/10.1063/1.1678153.

(4) Frisken, B. J. Revisiting the Method of Cumulants for the Analysis of Dynamic Light-Scattering Data. *Applied Optics* **2007**, *40* (24), 4087–4091. https://doi.org/10.1364/ao.40.004087.

(5) Punjani, A.; Rubinstein, J. L.; Fleet, D. J.; Brubaker, M. A. CryoSPARC: Algorithms for Rapid Unsupervised Cryo-EM Structure Determination. *Nat. Methods* **2017**, *14* (3), 290–297. https://doi.org/10.1038/nmeth.4169.

(6)   Emsley, P.; Lohkamp, B.; Scott, W. G.; Cowtan, K. Features and Development of Coot. *Acta Crystallographica Section D: Biological Crystallography* **2010**, *66* (4), 486–501. https://doi.org/10.1107/S0907444910007493.

(7)   Cho, H.; Choi, Y.; Min, K.; Son, J. B.; Park, H.; Lee, H. H.; Kim, S. Over-Activation of a Nonessential Bacterial Protease DegP as an Antibiotic Strategy. *Communications Biology* **2020**, *3* (1), 1–9. https://doi.org/10.1038/s42003-020-01266-9.

(8)   DiMaio, F.; Leaver-Fay, A.; Bradley, P.; Baker, D.; André, I. Modeling Symmetric Macromolecular Structures in Rosetta3. *PLoS ONE* **2011**, *6* (6), 1–13. https://doi.org/10.1371/journal.pone.0020450.

(9)   Pettersen, E. F.; Goddard, T. D.; Huang, C. C.; Couch, G. S.; Greenblatt, D. M.; Meng, E. C.; Ferrin, T. E. UCSF Chimera - A Visualization System for Exploratory Research and Analysis. *Journal of Computational Chemistry* **2004**, *25* (13), 1605–1612. https://doi.org/10.1002/jcc.20084.

(10)   Goddard, T. D.; Huang, C. C.; Meng, E. C.; Pettersen, E. F.; Couch, G. S.; Morris, J. H.; Ferrin, T. E. UCSF ChimeraX: Meeting Modern Challenges in Visualization and Analysis. *Protein Science* **2018**, *27* (1), 14–25. https://doi.org/10.1002/pro.3235.

(11)   Attri, A. K.; Fernández, C.; Minton, A. P. Self-Association of Zn-Insulin at Neutral PH: Investigation by Concentration Gradient-Static and Dynamic Light Scattering. *Biophysical Chemistry* **2010**, *148* (1–3), 23–27. https://doi.org/10.1016/j.bpc.2010.02.001.

(12)   Skórko-Glonek, J.; Zurawa, D.; Tanfani, F.; Scirè, A.; Wawrzynów, A.; Narkiewicz, J.; Bertoli, E.; Lipińska, B. The N-Terminal Region of HtrA Heat Shock Protease from Escherichia Coli Is Essential for Stabilization of HtrA Primary Structure and Maintaining of Its Oligomeric Structure. *Biochimica et Biophysica Acta - Proteins and Proteomics* **2003**, *1649* (2), 171–182. https://doi.org/10.1016/S1570-9639(03)00170-5.

(13)   Mechtler, K.; Ehrmann, M.; Kurt, J.; Huber, R.; Stingl, C.; Sawa, J.; Clausen, T.; Krojer, T.; Pangerl, K. Interplay of PDZ and Protease Domain of DegP Ensures Efficient Elimination of Misfolded Proteins. *Proceedings of the National Academy of Sciences* **2008**, *105* (22), 7702–7707. https://doi.org/10.1073/pnas.0803392105.